9250–9261 *Nucleic Acids Research, 2011, Vol. 39, No. 21* *Published online 22 August 2011*
doi:10.1093/nar/gkr635

Polynucleotide phosphorylase exonuclease and polymerase activities on single-stranded DNA ends are modulated by RecN, SsbA and RecA proteins

Paula P. Cardenas[1], Thomas Carzaniga[2], Sandro Zangrossi[3], Federica Briani[2], Esther Garcia-Tirado[1], Gianni Dehò[2,*] and Juan C. Alonso[1,*]

[1]Centro Nacional de Biotecnología (CNB-CSIC), Darwin 3, 28049 Madrid, Spain, [2]Università degli Studi di Milano, Via Celoria 26 and [3]Centro di Studio del CNR sulla Biologia Cellulare e Molecolare delle Piante, 20133 Milan, Italy

Received June 16, 2011; Revised July 18, 2011; Accepted July 19, 2011

ABSTRACT

Bacillus subtilis pnpA **gene product, polynucleotide phosphorylase (PNPase), is involved in double-strand break (DSB) repair via homologous recombination (HR) or non-homologous end-joining (NHEJ). RecN is among the first responders to localize at the DNA DSBs, with PNPase facilitating the formation of a discrete RecN focus per nucleoid. PNPase, which co-purifies with RecA and RecN, was able to degrade single-stranded (ss) DNA with a 3′ → 5′ polarity in the presence of Mn^{2+} and low inorganic phosphate (Pi) concentration, or to extend a 3′-OH end in the presence dNDP·Mn^{2+}. Both PNPase activities were observed in evolutionarily distant bacteria (*B. subtilis* and *Escherichia coli*), suggesting conserved functions. The activity of PNPase was directed toward ssDNA degradation or polymerization by manipulating the Pi/dNDPs concentrations or the availability of RecA or RecN. In its dATP-bound form, RecN stimulates PNPase-mediated polymerization. ssDNA phosphorolysis catalyzed by PNPase is stimulated by RecA, but inhibited by SsbA. Our findings suggest that (i) the PNPase degradative and polymerizing activities might play a critical role in the transition from DSB sensing to end resection via HR and (ii) by blunting a 3′-tailed duplex DNA, in the absence of HR, *B. subtilis* PNPase might also contribute to repair via NHEJ.**

INTRODUCTION

DNA double-strand breaks (DSBs) are highly cytotoxic lesions that arise spontaneously during growth or following exposure to DNA damaging agents, such as H_2O_2. The rapid detection and subsequent repair of DNA DSBs is critical for the survival of all living organisms. One-ended DSBs are repaired by homologous recombination (HR), whereas the two-ended DSBs are repaired by either HR or non-homologous end joining (NHEJ). HR relies on the presence of a homologous duplex template, whereas NHEJ directly rejoins the two ends of the broken chromosomes by ligation (1–7). NHEJ is error prone and can operate in any phase of the cell cycle in eukaryotes, but in bacteria only when a single chromosome copy is present, or when HR is impaired; therefore, only a minor fraction of two-ended DSBs are expected to be repaired by NHEJ. Whereas HR is error free and constrained to the S and G2 stages in eukaryotes, but is by far the major DSB repair avenue in bacteria (1,3,8,9).

In eukaryotes, among the first responder to DSBs is the MRX(N) complex constituted by Mre11, Rad50 and Xrs2 (in budding yeast) or Nbs1 (in mammals) (4,10). Then, the ends are processed to form the invasive 3′ single-stranded DNA (ssDNA) tails. This processing reaction occurs in two steps, a limited end resection by the MRX(N) complex in concert with Sae2 (CtIP in mammals) (11–14) followed by a processive resection of the 5′-end by the Sgs1(BLM)–Top3(TopoIIIα)–Rmi1(RMI1)–Dna2(DNA2) or Sgs1(BLM)–Exo1(EXO1)–MRX(MRN) complex to form a long 3′ ssDNA tail (long-range end processing) in the presence of the single-strand binding RPA protein

*To whom correspondence should be addressed. Gianni Dehò. Tel: +39 02 5031 5019; Fax: +39 02 5031 5044; Email: gianni.deho@unimi.it
Correspondence may also be addressed to Juan C. Alonso. Tel: +34 91585 4546; Fax: +34 91585 4506; Email: jcalonso@cnb.csic.es

The authors wish it to be known that, in their opinion, the first two authors should be regarded as joint First Authors.

(13–20). The 3′ ssDNA tail serves as the substrate for assembly of a Rad51 nucleoprotein filament that searches for the homologous duplex (3,7,21). In bacteria, the presence of a DSB (site-specific or randomly induced) in *rec*$^+$ cells re-localizes RecN from a diffuse distribution to a discrete focus per nucleoid to form a discrete repair center (RC) per nucleoid (9). In *Bacillus subtilis*, damage-induced RecN accumulation is readily detected 15–20 min after mitomycin C (MMC) treatment, followed by RecO, RecR and RecA co-localization with RecN-induced RC 10–15 min later (22). After damage recognition by RecN long tracts end resection to generate extensive 3′ single-stranded tails occurs via two routes. The AddAB (counterpart of RecBCD or AdnAB) helicase–nuclease complex or the RecJ ssDNA exonuclease, in concert with a RecQ-like helicase (RecQ or RecS simplified here as RecQ/RecS) and SsbA, process the DNA ends to generate a long 3′-tailed duplex bound by RecA (6,9,21,23). In the absence of processive end resection (in the *addAB* Δ*recJ* background) several RecN foci, rather than a single RC, are present per nucleoid and RecA threads are not observed (24).

Previous studies revealed that (i) at the DSB-induced foci, both eukaryotic MRX(N) and bacterial RecN increase the local concentration of damaged DNA ends by bridging and tethering them, leading to rosette-like structures *in vitro* (4,25,26); (ii) Mre11 degrades 3′ ends (an Mn^{2+}-dependent activity modulated by Rad50 and Xrs2) (11,12), whereas RecN lacks an end-resection activity (27); (iii) eukaryotic and bacterial Ku, the DNA end-binding subunit of the NHEJ machinery, act as negative regulators of long-range end resection by preventing both eukaryotic Exo1-dependent or bacterial AdnAB-dependent formation of long 3′ ssDNA tails (2,28–30); (iv) an Mn^{2+}-dependent 3′ → 5′ ssDNA exonuclease activity, which co-purifies with RecN, was recently attributed to polynucleotide phosphorylase (PNPase) (27); and (v) the Mre11 or the PNPase activity is dispensable when enzymatic 'ligatable' breaks are generated (15,17,27).

PNPase (encoded by *pnpA* in *B. subtilis* or *pnp* in *Escherichia coli*) is a non-essential multifunctional protein, responsible for Mg^{2+}- and inorganic phosphate (Pi)-dependent 3′ → 5′ processive phosphorolytic degradation of RNA, and template-independent polymerization of rNDPs into RNA (31–36). PNPase, which is generally thought of as an enzyme dedicated to RNA metabolism (37,38), in the presence of either Mn^{2+} or Fe^{3+} ions may catalyze template-independent polymerization of dNDPs into ssDNA (39–41). Genetic evidences implicates *pnpA (pnp)* in the repair of H_2O_2 damage both in *B. subtilis* and *E. coli* (27,42), and this effect might be direct because in *pnpA* cells there are no significant difference in the relative amounts of transcripts of genes involved in DNA repair and/or repair-by-recombination (27). *In vivo* analyses revealed that a null *B. subtilis pnpA* (Δ*pnpA*) mutation is epistatic to Δ*recN* or Δ*ku* mutations, which by themselves are non-epistatic, whereas Δ*pnpA* is non-epistatic to *addA* or Δ*recJ* (27). *In vitro B. subtilis* PNPase (PNPase$_{Bsu}$), which co-purifies with RecN, has an Mn^{2+}-dependent 3′ → 5′ exodeoxyribonuclease activity (27). This raises new questions as to whether this multifaceted enzyme is directly implicated in DNA metabolism during DSB repair in bacteria and suggests an early involvement of PNPase after a DSB.

To shed light on the molecular mechanism underlying the transition from RecN DSB sensing to the generation of the recombinogenic 3′-ssDNA ends, we characterized the PNPase enzymes from *B. subtilis* and *E. coli* (PNPase$_{Bsu}$ and PNPase$_{Eco}$), respectively, and the effects of RecN, RecA and SsbA on PNPase$_{Bsu}$ enzymatic activities. *E. coli* and *B. subtilis* are separated by more than 1.5 billion years, a time divergence larger than the one between humans and plants. It is thus likely that any conserved PNPase activity should be present in most bacteria.

MATERIALS AND METHODS

Bacterial strains and plasmids

All *B. subtilis* strains used are isogenic with the *rec*$^+$ control (BG214) *trpC*2 *metB*5 *amyE sigB*37 *xre*1 *att*SPβ *att*ICE*Bs*1. *B. subtilis recN:yfp* DNA (BG1089) was used to transform the isogenic derivative Δ*pnpA* (BG993) (27), rendering *recN:yfp* Δ*pnpA* (BG1091). The 5′-end of the *B. subtilis pnpA* gene was fused to the *gfp* gene leading to *gfp:pnpA* fusion (pCB800). Linearized pCB800 DNA was used to transform *rec*$^+$ (BG214) and its isogenic Δ*pnpA* derivative (BG993) into the *amy* locus, rendering BG1167 (*rec*$^+$ *gfp:pnpA*) and BG1169 (Δ*pnpA gfp:pnpA*). The *gfp:pnpA* fusion failed to complement the Δ*pnpA* mutation of strain BG1169. The BG214 strain or *E. coli* BL21(DE3) strain were used for protein overexpression.

Plasmid pAZ101 and pGM742 have been previously described (43,44). Plasmids pCB890-borne *pnpA*R399D R400D and pCB891-borne *pnpA*D493G encode a modified *pnpA* gene that was constructed by site-directed mutagenesis: CGT of wild type (wt) codons 399 and 400, coding for Arg, was exchanged against GAT that codes for Asp in the expressed protein variant PNPase$_{Bsu}$R399D R400D equivalent to PNPase$_{Eco}$R398D and R399D and GAC of wt codon 493, coding for Asp, was exchanged against GGC that codes for Gly in the expressed protein variant PNPase$_{Bsu}$D493G equivalent to PNPase$_{Eco}$D492G (see 45).

Reagents and protein purification

All chemicals used were reagent grade, dithiothreitol (DTT), rNTPs, dNTP, rNDPs, dNDPs and ddTTP were purchased from Sigma or Promega and [γ-^{32}P]ATP from Amersham Bioscience and then Perkin Elmer. The ssDNA and dsDNA concentrations were measured using extinction coefficients of 1.54×10^{-4} and $8780\ M^{-1}cm^{-1}$ at 260 nm, respectively. The 60-nt long ssDNA used were: 5′-AGCT(A)$_{56}$-3′ (oligo-A56), 5′-AGGCCTCCCGGGA TCCGCTAGCAGGAGGAAATTCACCATGGGTAA AGGAGAAGAACTTTT-3′ (oligo-A) and 5′- CTCCTA TTATGCTCAACTTAAATGACCTACTCTATAAAG CTATAGTACTGCTATCTAATC-3′ (oligo-F). The 20-nt long oligos complementary to oligo-A at positions 1–20 (oligo-B) and at positions 21–40 (oligo-C) or non-complementary with oligo-A (5′-AGTGACTTTAG TACAGTACC, oligo-E), and the 30-nt long ssDNA

complementary to oligo-A at positions 40–60 with a 10-nt overhang (5′-ATGAACCTACGAAAAGTTCTTCTCCT TTAC-3′ (oligo-D), 10 μM each, were annealed to oligo-A (5 μM) in 50 mM Tris–HCl (pH 7.5), 50 mM NaCl, by heating for 5 min at 95°C and slow cooling at room temperature. The 60-nt long oligo-F ssDNA was extended using terminal transferase (Roche) and ddTTP; to reduce to a negligible level the proportion of the oligo with a 3′-OH end, two sequential extension reactions were performed, to render a 61-nt long oligo-F′ ssDNA. The 107-, 105- and 102-bp dsDNA fragments with a 3′ protruding, blunt or 5′ protruding end, respectively, were obtained by PCR amplification of the multiple cloning site of pGM742 with with primers FG953 (CCTGTTTGATG GTGGTTCGGTACG) and FG125 (GACCGCTTCTGC GTTCTGATT), cleaved by either KpnI (3′-protruding), SmaI (blunt) or BamHI (5′-protruding) restriction enzyme, and gel purified. The dsDNA fragments were incubated with 10 nM PNPase$_{Eco}$ or PNPase$_{Bsu}$ in buffer A containing 100 μM dADP for the time indicated at 26°C. The 60- or 61-nt long ssDNA and the dsDNAs were 5′-end-labeled using [γ-^{32}P]-ATP and T4 polynucleotide kinase (New England Biolabs) purified [from the non-incorporated nucleotide] by Sephadex G50 gel filtration. Uniformly labeled [^{32}P]-RNA substrate was synthesized by *in vitro* transcription with T7 RNA polymerase and [α-^{32}P]-CTP using a DNA template obtained by PCR amplification of plasmid pAZ101 with oligonucleotides FG1626 (taatacgactcactatagggCATTAGCCGCGCGAACCTC, where lowercase letters indicate the T7 promoter, and uppercase letters indicate *E. coli* sequence) and FG1627 (GAATGATCTTCCGTTGCAGAG) (46).

PNPase$_{Eco}$, PNPase$_{Bsu}$ and SsbA were over-expressed in *E. coli* BL21(DE3) cells bearing plasmid borne *pnp*, *pnpA* or *ssbA* genes, purified and stored as previously described (46–48). RecA and RecN were over-expressed in *B. subtilis* BG214 cells bearing plasmid borne *recA* or *recN* gene, purified and stored as previously described (49,50). PNPase$_{Bsu}$R399D R400D and PNPase$_{Bsu}$D493G variants were purified using as previously described for PNPase$_{Bsu}$ (47).

Assays of PNPase activities

The 5′-end [^{32}P]-labeled oligo-A56 or oligo-A ssDNA (0.25 nM in molecules) was incubated with PNPase$_{Eco}$ or PNPase$_{Bsu}$ (10 nM) in buffer A [10 mM Tris–HCl (pH 7.5), 10 mM KCl, 2 mM $MnCl_2$, 0.75 mM DTT, 2% PEG-6000], buffer B (as buffer A but with 2 mM $MgCl_2$ instead of $MnCl_2$) or buffer C (as buffer A but lacking $MnCl_2$) containing the indicated concentration of dADP, dCDP, dGDP, dTDP, rATP or dATP, or no nucleotide, with the indicated concentrations of sodium phosphate. The 5′-end labeled [^{32}P]-ssDNA was pre-incubated with RecN and then with increasing concentrations of PNPase$_{Bsu}$ in buffer A containing the indicated concentration of dADP and rATP or dATP. The samples were separated on denaturing 6% or 12% (as indicated) polyacrylamide gel electrophoresis (dPAGE) (46).

Thin layer chromatography of the radiolabeled DNA degradation products was performed on polyethyleneimine–cellulose (PEI) plates with buffer D [0.4 M K_2HPO_4 (pH 8.0), 0.7 M H_3BO_3] as the mobile phase as described (51).

Image acquisition

To exponentially growing cells (OD_{560} = 0.5) 50 ng ml^{-1} of MMC was added and the culture was incubated for 30 min. The cells were collected, the DNA was stained with 4′,6-diamidino-2-phenylindole (DAPI; final concentration 0.2 μg ml^{-1}) and fluorescence microscopy was performed as described (22).

RESULTS

Absence of PNPase abrogates formation of a discrete RecN focus per nucleoid

DNA-damage response recruits complex molecular machinery involved in DNA repair to DSBs. *In vivo, B. subtilis* RecN is among the first responders leading to the formation of a discrete RC per nucleoid (22), and a null *pnpA* (Δ*pnpA*) mutation is epistatic to Δ*recN* (27). *In vitro*, RecN-bound (d/r)ATP recognizes ssDNA ends and tethers them onto a nucleoprotein complex, rosette-like structure (26,50). To determine whether PNPase$_{Bsu}$ acts in concert with RecN, the fate of the RecN:YFP protein was studied by fluorescence microscopy in *pnpA*$^+$ and Δ*pnpA* strains expressing a *recN*:*yfp* fusion upon MMC treatment. RecN:YFP appeared evenly distributed within the cells in both *pnpA*$^+$ and Δ*pnpA* exponentially growing cultures (Figure 1). Thirty minutes upon addition of MMC (50 ng ml^{-1}), DNA damage-induced RecN foci were detected in both *pnpA*$^+$ (72%, n = 808) and Δ*pnpA* (70%, n = 491) cells (Figure 1). *pnpA*$^+$ cells generally contained a discrete RecN:YFP focus per nucleoid in the majority of cells (~69%, n = 580), whereas two or more foci were rarely observed (~3% of the cells) (22) (Figure 1A). In contrast, a large fraction of Δ*pnpA* cells contained two (37%, n = 350) or multiple foci that appeared patchy (11%, n = 350), whereas a discrete focus was observed in ~22% of the cells (Figure 1B). RecN:YFP can thus form foci at DSBs early upon DNA damage in the absence of PNPase$_{Bsu}$, whereas the efficient formation of a single RC appears to require an active PNPase$_{Bsu}$ enzyme.

We also monitored the distribution of GFP-tagged PNPase$_{Bsu}$ in the absence and presence of MMC (Supplementary Figure S1). In ~80% of the cells (n = 665 cells), GFP:PNPase$_{Bsu}$ was found either to form foci at the cell poles (14–18%) (Supplementary Figure S1A, left panels), or distributed within the cell (Supplementary Figure S1B) in a way that was reminiscent of the filamentous helical structures (62–66%) previously described for *E. coli* PNPase (52); the remaining fraction showed fluorescence distributed throughout the cells or no fluorescence at all. The frequency of foci and helical structures (14–18% and 62–66%, respectively), however, was the about same both in untreated exponentially growing cells and upon addition of MMC.

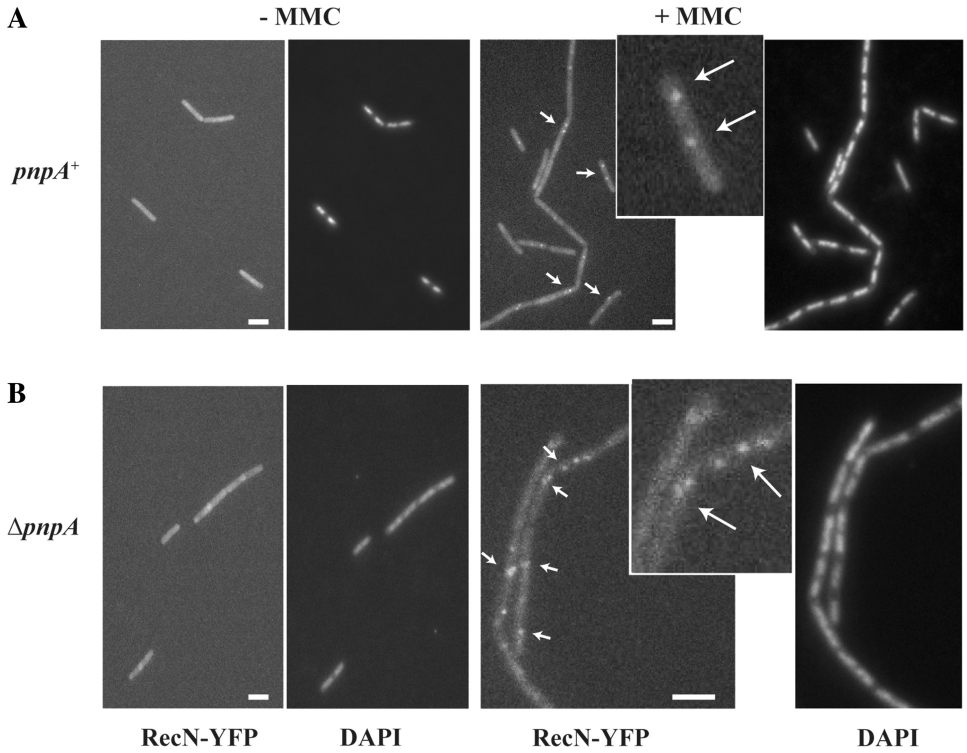

Figure 1. PNPase promotes assembly of a discrete RecN focus per nucleoid. *Bacillus subtilis* BG1089 (*pnpA*$^+$ *recN*:*yfp*) (**A**) and BG1091 (Δ*pnpA recN*:*yfp*) (**B**) exponentially growing cells were treated (+MMC, 50 ng/ml) or not (−MMC) for 30 min. The nucleoids were stained with DAPI and the intracellular distribution of RecN:YFP and DAPI was observed by fluorescence microscopy. The arrows indicate some MMC-induced foci. White bars 2 μm.

PNPase$_{Eco}$ catalyzes Mn^{2+}-dependent phosphorolysis

PNPase$_{Bsu}$ is an Mn^{2+}-dependent $3' \rightarrow 5'$ ssDNA exonuclease (27). To shed light into the role of PNPase in DNA processing, we compared *in vitro* exonucleolytic DNA degradation by purified *E. coli* and *B. subtilis* enzymes on a 60-nt long ssDNA potentially forming secondary structures (oligo-A) or an unstructured (oligo-A56) ssDNA. Both PNPases degraded oligo-A56 ssDNA with a $3' \rightarrow 5'$ polarity in the presence of Mn^{2+} and low Pi (10 μM) (Figure 2A, lanes 3–12 and 3A). Independent of protein concentration, PNPase$_{Eco}$ could run through the entire molecule whereas PNPase$_{Bsu}$ could not proceed more than ~25-nt (Figure 3B, lanes 4–6 and 10–12). When oligo-A ssDNA (Figure 3D) was used, PNPase$_{Bsu}$ only nibbled off 2-nt, whereas PNPase$_{Eco}$ could run through the entire molecule, although pausing at preferential sites (Figure 2B and 3C, lanes 3–5 and 8–10). Such differences could not be imputed to different specific activities of the two PNPase preparations, as no similar effects were observed when RNA was degraded (Supplementary Figure S2). Overall these data suggest that PNPase$_{Bsu}$ is less processive or efficient at DNA degradation and more sensitive to DNA secondary structures than PNPase$_{Eco}$.

ssDNA degradation occurred in the presence of low or even in the absence of supplemented Pi (27) (Figure 3A). This was likely due to contaminating Pi, since degradation of [α-^{32}P]-dATP uniformly labeled DNA by PNPase generated dADP both with and without added Pi, as shown by thin layer chromatography (Supplementary Figure S3). Thus PNPase promoted genuine ssDNA phosphorolysis. Unlike RNA phosphorolysis, which occurs at Pi concentrations as high as 10–30 mM (53), the Mn^{2+}-dependent DNase activity of both PNPases was completely inhibited by 100 μM or higher Pi concentrations (27) (Figure 2C). No ssDNA degradation could be detected when Mn^{2+} was replaced by Mg^{2+} (27) (Supplementary Figure S4A, lanes 3–12).

Bacterial PNPase catalyzes template-independent dNDP polymerization into ssDNA

In the presence of Mn^{2+} and dADP, both PNPases catalyzed template-independent ssDNA polymerization on both unstructured oligo-A56 and structured oligo-A ssDNA (Figure 2A and B). High dADP concentrations (1 mM) (or contaminating Pi possibly present in dADP commercial stocks), however, inhibited polymerization (Figure 2C, lanes 19 and 25).

In the presence of Mg^{2+}, template-independent polymerization occurred with a much lower efficiency than with Mn^{2+} (compare Figure 2, lanes 13–22 with Supplementary Figure S4A, lane 13–22). PNPase$_{Eco}$ was able to catalyze template-independent polymerization with oligo-A as a primer in the presence of Fe^{3+}, confirming a previous report (41), although less efficiently than with Mn^{2+} (compared Figure 2B, lanes 13–17 with

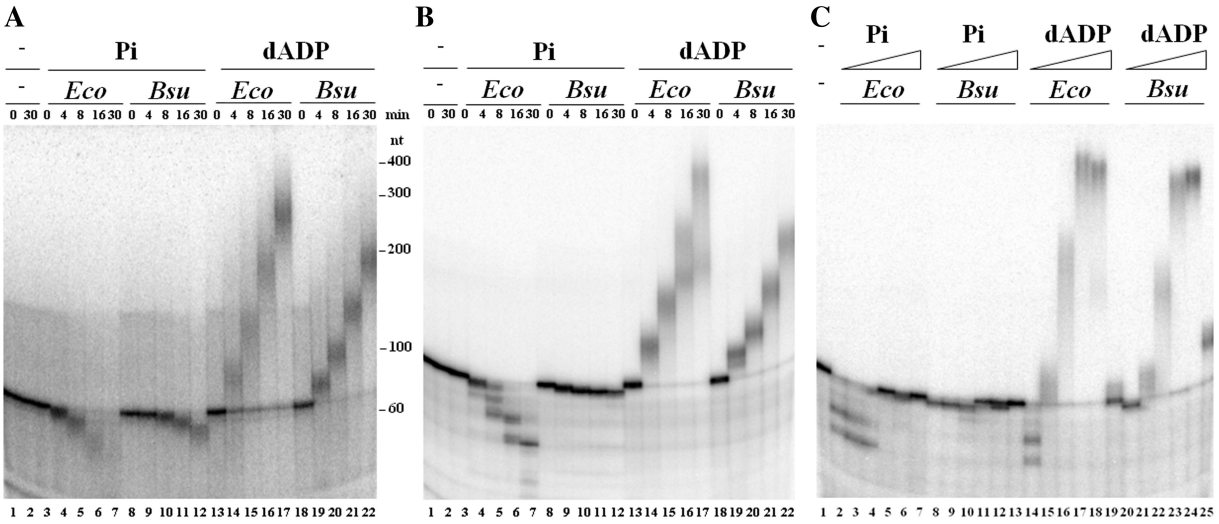

Figure 2. Mn^{2+}-dependent phosphorolysis, template-independent synthesis of ssDNA catalyzed by PNPase, and inhibition of phosphorolysis and polymerization by high concentrations of Pi and dADP, respectively. (**A**) [^{32}P]-oligo-A56 or (**B**) [^{32}P]-oligo-A (0.25 nM each) was incubated with $PNPase_{Eco}$ (*Eco*) or $PNPase_{Bsu}$ (*Bsu*) (10 nM) in buffer A containing either Pi (10 μM) or dADP (100 μM) for the time indicated (min) at 26°C. (**C**) The 5′-end labeled [^{32}P]-oligo-A (0.25 nM) was incubated with $PNPase_{Eco}$ or $PNPase_{Bsu}$ (10 nM each) in buffer A containing increasing Pi (0, 0.001, 0.01, 0.1, 1 and 10 mM) or dADP (0, 0.001, 0.01, 0.1, 1 and 10 mM) concentrations for 30 min at 26°C. The reaction products were fractionated by 6% dPAGE.

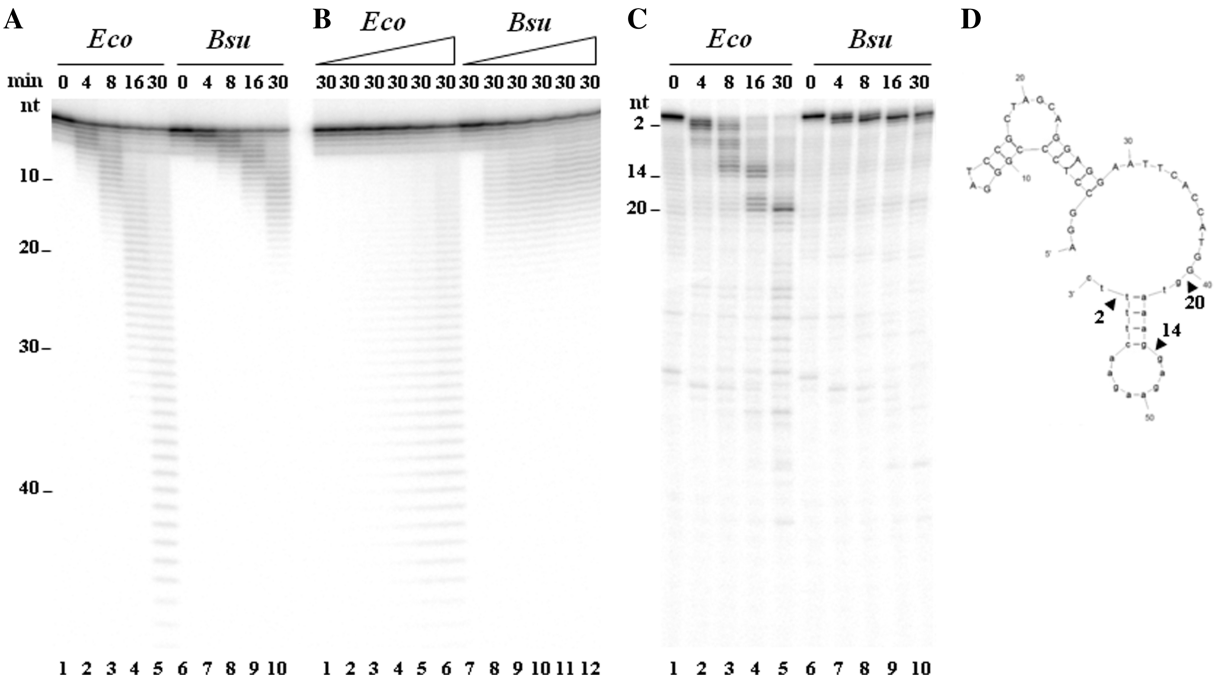

Figure 3. Phosphorolysis of different ssDNA probes by $PNPase_{Eco}$ (*Eco*) and $PNPase_{Bsu}$ (*Bsu*). The 5′-end labeled [^{32}P]-oligo-A56 (panels **A** and **B**) or [^{32}P]-oligo-A (**C**) (0.25 nM each) was incubated with $PNPase_{Eco}$ or PNPase in buffer A with 10 μM Pi for the times indicated at 26°C. PNPase was 10 nM (panels A and C) or at increasing concentrations (0, 0.5, 1, 2.5, 5 and 10 nM) (B). The reaction products were fractionated by 12% dPAGE. (**D**) M-FOLD-predicted secondary structure of oligo-A. The arrowheads denote the pausing sites.

Supplementary Figure S4A, lanes 2–7). When Fe^{3+} was replaced by Fe^{2+} polymerization was almost negligible (Supplementary Figure S4B). PNPase-mediated polymerization reaction was inhibited when Fe ions exceeded the 0.5 mM concentration (Supplementary Figure S4B).

All four dNDPs could be used as substrates for polymerization, although with different reaction rates, for both PNPases (dCDP ≈ dADP >> dTDP ≈ dGDP) (Supplementary Figure S5).

Polymerization of dADP by PNPase was stimulated by sub-stoichiometric concentrations of rADP but at equimolar or higher concentrations rADP exerted a negative effect (Supplementary Figure S6). In such conditions rADP was incorporated into co-polymers, as shown

by alkali degradation of the polymerization products (Supplementary Figure S6).

To unambiguously determine the function of PNPase and to examine whether the amino acids important for RNA phosphorolysis and NDP polymerization activities were also important for ssDNA phosphorolysis and dNDP polymerization we created two site-specific PNPase$_{Bsu}$ mutants. The PNPase$_{Bsu}$R399D R400D and PNPase$_{Bsu}$D493G variants, which correspond to the catalytically inactive PNPase$_{Eco}$R398D R399D and PNPase$_{Eco}$D492G proteins, respectively (45), were purified in parallel with wt PNPase, using the same purification protocol. Both PNPase$_{Bsu}$ mutant proteins were unable to catalyze degradation or template-independent ssDNA polymerization even when the mutant variants were present at a 1000-fold higher concentration than wt PNPase$_{Bsu}$ (Supplementary Figure S7). These data indicate that both RNA and ssDNA share the same catalytic site.

Bacterial PNPase can process a 3′-tailed duplex

To test whether PNPase was able to process duplex DNA with a 3′-protruding or recessed end, oligo-A ssDNA was annealed with a 2-fold excess of oligos complementary to different portions of the labeled probe (oligo-B, -C or -D) or the mock non-complementary oligo-E (Figure 4). PNPase$_{Eco}$ degraded 40-nt (A:B) or 20-nt (A:C) long 3′-protruding ends, but failed to degrade 3′-recessed ends (A:D) (Figure 4A, lane 16–20).

Both PNPases extended dsDNA digested with a restriction enzyme leaving a 4-nt long 3′-protruding, a blunt

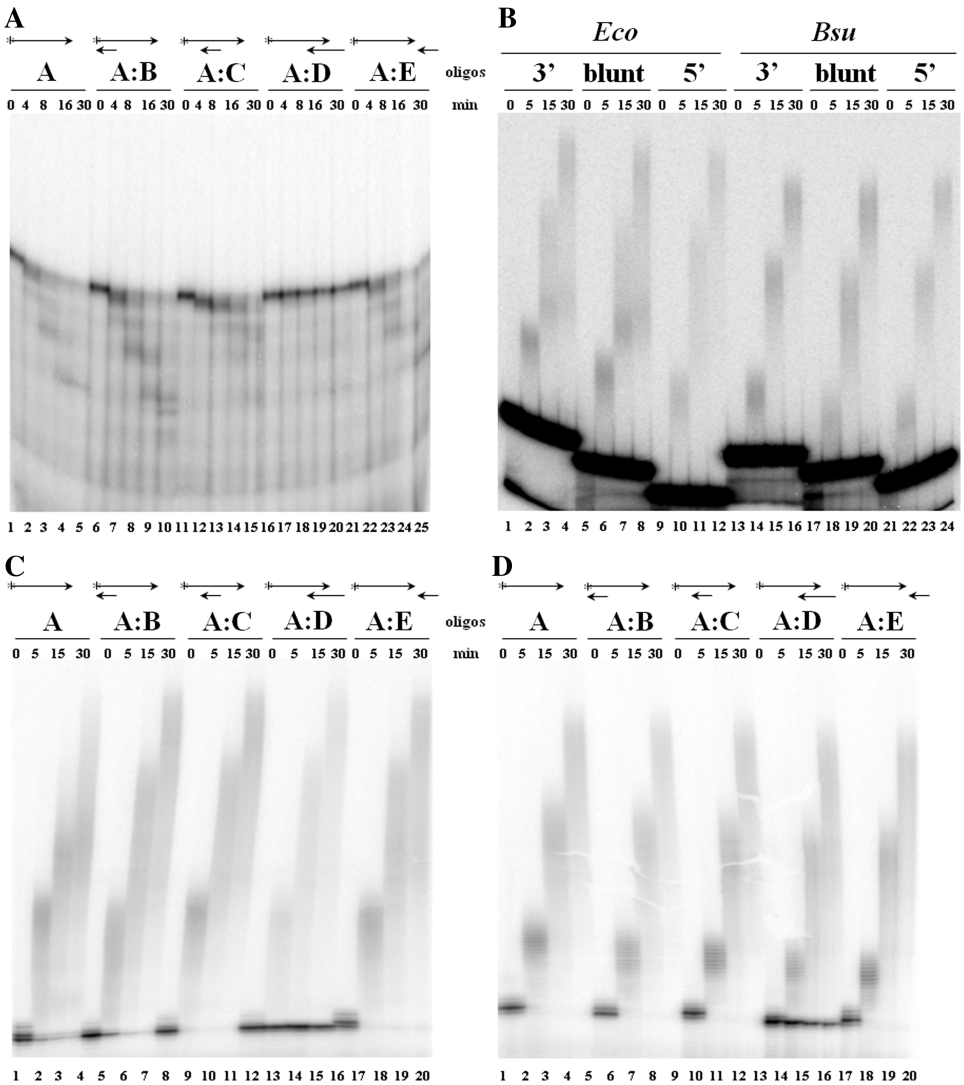

Figure 4. PNPase catalyzed phosphorolysis of and template-independent polymerization on duplex DNA with different 3′-ends. The 5′-end labeled [^{32}P]-oligo-A (0.25 nM) alone, annealed with non-labeled complementary oligo-B (A:B), -C (A:C) or -D (A:D) (0.50 nM each), or together with oligo-E as depicted on top of panels A, C and D were incubated with 10 nM PNPase$_{Eco}$ in buffer A containing 10 μM P_i (**A**) with 10 nM PNPase$_{Eco}$ (**C**) or PNPase$_{Bsu}$ (**D**) in buffer A containing dADP (100 μM) for the time indicated at 26°C. (**B**) 5′-end labeled [^{32}P]-dsDNA with either 3′-protruding, blunt or 5′-protruding end was incubated with 10 nM PNPase$_{Eco}$ (*Eco*) or PNPase$_{Bsu}$ (*Bsu*) in buffer A containing 100 μM dADP for the time indicated at 26°C. Samples were separated as in Figure 2.

end or a 5′- protruding end (Figure 4B). Template-independent ssDNA polymerization by PNPase was significantly enhanced if the length of the tailed ssDNA was increased. Both PNPase$_{Eco}$ (Figure 4C) and PNPase$_{Bsu}$ (Figure 4D) efficiently extended the 3′-protruding ends of partially dsDNA substrates. Elongation, however, was less efficient with a 3′-recessed end (A:D) substrate. PNPase$_{Bsu}$ seemed to be more proficient than PNPase$_{Eco}$ with this substrate (Figure 4C and D). The lower efficiency of polymerization with a dsDNA primer with short or no tail as compared with the partially dsDNA oligos (Figure 4C and D) might depend on the lower affinity of PNPase for dsDNA (27,54) and the preference for a ssDNA tail as primer.

rATP and dATP modulate the PNPase activities

Biochemical analyses revealed that (d/r)ATP is an allosteric inhibitor of PNPase$_{Eco}$ RNA degradation and polymerization activities (46) and of PNPase$_{Bsu}$ ssDNA degradation activity (27). To address whether (d/r)ATP affected both PNPase activities on ssDNA, assays were performed in the presence of (d/r)ATP•Mn^{2+}. PNPase ssDNA degradation was inhibited by the presence of 1 mM rATP•Mn^{2+}, and addition of even lower rATP concentrations (100 μM) also inhibited dADP polymerization (Supplementary Figure S8A). Likewise, dATP inhibited both phosphorolysis and polymerization by PNPase (Supplementary Figure S8B). Interpretation of such results is complicated by the fact that r/dNTPs are unavoidably contaminated by Pi and r/dNDPs (see Supplementary Figure S3, lanes 5 and 6), which by themselves modulate PNPase activities. This, however, could not explain the inhibitory effect in both directions by the same nucleotide preparation; moreover, the inhibitory effects of dATP was observed at very low dATP concentrations (10 and 1 μM for degradation and polymerization, respectively) versus concentrations of 10 μM Pi and 100 μM dADP as substrates, where concentration of degradation byproducts may be negligible. In addition, although contaminating Pi might directly inhibit degradation of ssDNA (see above), this is considered unlikely because contaminating Pi concentrations of 100 μM or higher are needed for inhibition of the degradative activity (see above). Thus inhibition of PNPase by r/dATP seems the more reasonable explanation of the bulk of these data.

RecN and SsbA modulate PNPase polymerization into ssDNA

In vivo analyses in *B. subtilis* revealed that DNA damage-induced RecN to form a discrete focus per nucleoid (22). *In vitro*, RecN is a ssDNA-dependent (r/d)ATPase (50). In the (r/d)ATP or (r/d)ADP bound form, RecN, assembles at the 3′-OH ends to form large networks with ssDNA molecules (rosette-like structures) that are insensitive to ExoIII degradation (26,50). Addition of SsbA (counterpart of *E. coli* SSB or eukaryotic RPA) does not disrupt the rosette-like structures (26). As shown in Figure 1, PNPase$_{Bsu}$, which co-purifies with RecN (27), altered the formation of a discrete RecN focus per nucleoid. As we failed to detect stable physical PNPase$_{Bsu}$ and RecN interactions in solution using co-immunoprecipitation or protein cross-linking methodologies, we tested whether RecN could modulate any of the PNPase activities.

RecN alone neither polymerized ssDNA (Figure 5A, lane 3) nor degraded ssDNA (27). RecN had two different effects on PNPase-mediated template-independent polymerization. First, RecN•dATP stimulated ~6-fold ssDNA extension when incubated with limiting PNPase$_{Bsu}$ concentrations (e.g. as low as 0.2 nM) (Figure 5A and B). Second, the presence of RecN abolished the inhibitory effect exerted by 1 mM dATP on dADP polymerization (Figure 5A and B, lane 13). It is possible that RecN-mediated rosette-like structures facilitate PNPase$_{Bsu}$ access to a high local concentration of ssDNA ends, and that RecN catalyzed dATP hydrolysis, rather than any other ssDNA-dependent dATPase, contributed to the observed stimulation. As expected RecN failed to activate the catalytic site mutants

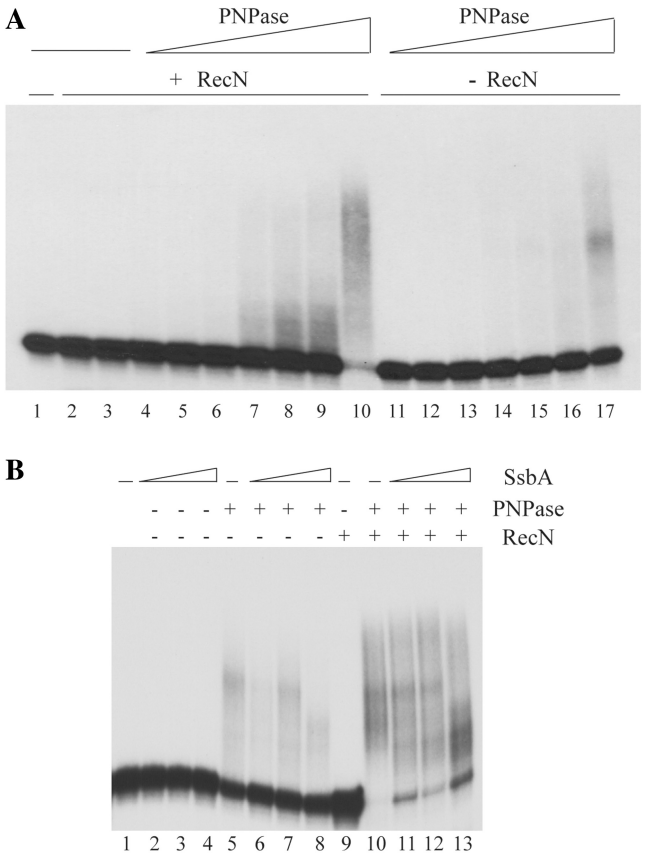

Figure 5. PNPase activities are modulated by RecN and SsbA. (**A**) The 5′-end labeled [^{32}P]-oligo-F ssDNA (0.25 nM) was pre-incubated with or without RecN (10 nM), as indicated, in buffer A containing 1 mM dATP and 100 μM dADP for 5 min. Then increasing concentrations of PNPase$_{Bsu}$ (7, 12, 25, 50, 100, 200 500, 750 or 1000 pM) were added and the reaction incubated for 30 min at 26°C. In lane 2, dADP was omitted. (**B**) The 5′-end labeled [^{32}P]-oligo-F (0.25 nM) was pre-incubated with or without RecN (10 nM) for 5 min in buffer A containing 1 mM dATP at 26°C. PNPase$_{Bsu}$ (0.5 nM) and 100 μM dADP was added, 5 min later different SsbA concentrations (0.75, 1.5 and 3 nM) were added and the reaction incubated for 20 min at 26°C. + and −, denote the presence or absence of the indicated protein. Samples were separated as in Figure 2.

PNPase$_{Bsu}$R399D R400D or PNPase$_{Bsu}$D493G (Supplementary Figure S7A).

RecN binds to the ssDNA ends in a dATP-dependent manner and tethers and bridges them, and such rosette-like structures are insensitive to SsbA addition (26,50). SsbA, at stoichiometric concentrations (1 SsbA tetramer/80-, 40- or 20-nt), showed a significant inhibitory effect on PNPase-catalyzed ssDNA polymerization when compared with the absence of SsbA (Figure 5B, lane 5 versus 6–8). In the presence of RecN•dATP, SsbA inhibited PNPase$_{Bsu}$ polymerizing activity less severely (Figure 5B, lanes 6–8 versus 11–13).

RecA and SsbA modulate PNPase degradation of ssDNA

In the presence (d/r)ATP•Mg^{2+}, RecA assembles onto ssDNA to form an extended RecA•ssDNA filament and promotes strand exchange with homologous dsDNA, whereas in the apo form or in the presence of ADP, RecA can bind ssDNA and form a compact filament inactive for RecA-mediated DNA strand exchange (55,56). RecA catalyzes the hydrolysis of dATP and, to a lesser extent, rATP in a ssDNA-dependent manner (48,57). PNPase$_{Eco}$ co-purifies with RecA$_{Eco}$ (58) and an interaction between both proteins was predicted (www.compsysbio.org/bacteriome). We failed, however, to detect a stable physical interaction between *B. subtilis* PNPase and RecA proteins, although an *in vivo* interaction between PNPase and the RecA-like domain of an RNA helicase was documented by a two-hybrid system (59). To determine whether RecA or RecA and SsbA affect the PNPase$_{Bsu}$ activities, we tested the ability of PNPase$_{Bsu}$ to degrade ssDNA or to polymerize into ssDNA. In the apo or in the nucleotide-bound form RecA, at stoichiometric concentrations (1 RecA/3-nt), neither degrades (see also Figure 6B) nor stimulates template-independent polymerization into ssDNA (21,60). As shown above (Figures 2B and 3C) PNPase$_{Bsu}$ could nibble only a few nucleotides of the structured ssDNA substrate. At very low Pi concentration (no exogenously added Pi), RecA markedly stimulated PNPase-catalyzed ssDNA phosphorolysis >10-fold, leading to extensive degradation of the probe (Figure 6A, compare lanes 2–4 with 8–10). ssDNA degradation by

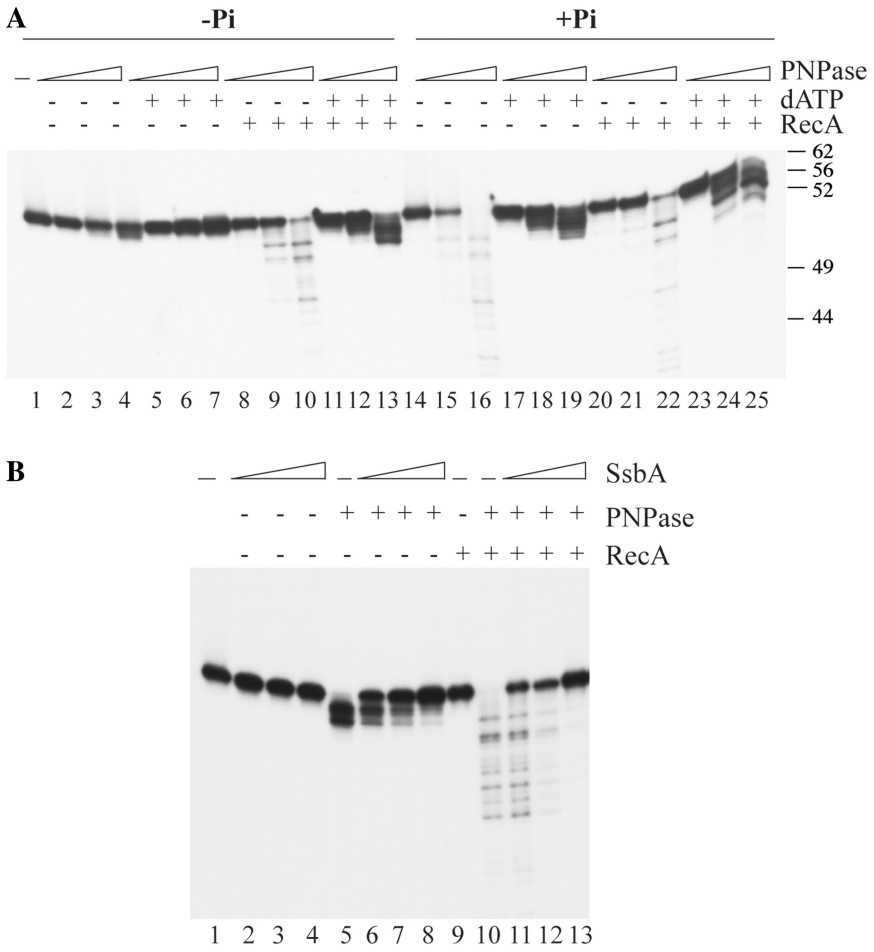

Figure 6. PNPase activities are modulated by RecA and SsbA. (**A**) The 5′-end labeled [^{32}P]-oligo-F ssDNA (0.25 nM) was pre-incubated with or without RecA (20 nM) in buffer A containing or not P_i (10 μM) and/or dATP (1 mM), as indicated, for 5 min at 26°C. Then increasing concentrations of PNPase$_{Bsu}$ (0.1, 0.5 and 1 nM) were added and the reaction incubated for 30 min. + and −, denote the presence or absence of the indicated protein. (**B**) The 5′-end labeled [^{32}P]-oligo-F (0.25 nM) was pre-incubated with different SsbA concentrations (0.75, 1.5 and 3 nM) in buffer A for 5 min. Then RecA (20 nM) was added and 5 min later PNPase$_{Bsu}$ (10 nM) and the reaction incubated for 30 min at 26°C. + and −, denote the presence or absence of the indicated protein. Samples were separated as in Figure 2.

PNPase$_{Bsu}$ accumulates dNDPs, hence we could not discriminate whether RecA exerted the stimulatory effect on PNPase-mediated ssDNA degradation in the apo or in the dADP-bound form.

dATP, which is critical for the formation of an active RecA•ssDNA filament (48,57), limited the extent of PNPase-mediated 3′-end resection (Supplementary Figure S8, lanes 6 and 12). dATP also limited the stimulatory effect exerted by RecA on DNA resection at low Pi concentration and reduced ssDNA degradation in 10 μM Pi (Figure 6A, lanes 11–13 and 23–25). These data suggest that RecA stimulates ssDNA degradation by PNPase$_{Bsu}$ perhaps by melting out secondary structures in the DNA, but RecA fails to overcome the inhibitory effect exerted by dATP on PNPase-mediated 3′-end resection. It is also possible that the products of RecA-mediated dATP hydrolysis and accumulation of Pi concentration higher than 10 μM might limit the extent of degradation. The catalytic site mutants PNPase$_{Bsu}$R399D R400D or PNPase$_{Bsu}$D493G could not be activated by the addition of RecA (Supplementary Figure S7B).

Addition of RecA in the apo bound form facilitated full degradation of the ssDNA substrate (Figure 6B, lanes 5 and 10). Addition of SsbA (1 SsbA tetramer/80-, 40- or 20-nt) inhibited PNPase$_{Bsu}$ degradation of ssDNA (Figure 6B, lanes 6–9). Similar inhibition was observed in the presence of RecA. It is likely that SsbA (1 SsbA tetramer/20-nt) inhibits PNPase-mediated degradation of ssDNA and RecA, in the apo or dADP-bound form, cannot overcome such inhibitory effect (Figure 6B, lanes 11 and 13). It is likely that SsbA poses a barrier to PNPase-mediated degradation of ssDNA.

RecA stimulates PNPase degradation of ssDNA

To examine whether RecA affected PNPase$_{Bsu}$ degradation of a ssDNA lacking a 3′OH end we extended the 60-nt ssDNA with ddTTP, rendering a 61-nt long ssDNA with a ddTMP incorporated at the 3′-end. When the 60-nt long ssDNA with a 3′-OH end was used, PNPase$_{Bsu}$ only nibbled off 2-nt (Figure 7, lane 2–4), confirming that PNPase$_{Bsu}$ is sensitive to DNA secondary structures (Figure 3D). On the contrary, PNPase$_{Bsu}$ failed to degrade the 3′-deoxy 61-nt long ssDNA (Figure 7, lanes 6–8); however, the presence of RecA stimulated PNPase-catalyzed phosphorolysis of 3′-deoxy-terminated ssDNA (Figure 7, lanes 9–11). It thus appeared that PNPase$_{Bsu}$ can degrade a 3′-end lacking a 3′-OH group on its sugar moiety in the presence of RecA.

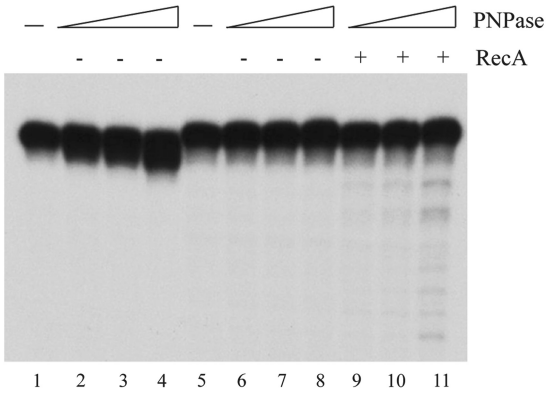

Figure 7. RecA stimulates phosphorolysis of ssDNA with a 3′-ddTMP. The 60-nt long 5′-end labeled [^{32}P]-oligo-F (0.25 nM, lanes 1–4) or the 61-nt long 5′-end labeled [^{32}P]-oligo-F' with a ddTMP at the 3′-end (0.25 nM, lanes 5–11) was pre-incubated with PNPase$_{Bsu}$ (0.5, 1 and 5 nM) for 5 min in buffer A. Then RecA (20 nM) was added and the reaction incubated for 30 min. The samples were separated as in Figure 2.

DISCUSSION

In this study, we biochemically characterized the Mn^{2+}-dependent $3' \rightarrow 5'$ phosphorolytic degradation of ssDNA and template-independent polymerization of dNDPs into ssDNA activities of *E. coli* or *B. subtilis* PNPase (27, this work). PNPase, which is a multifunctional enzyme, is also responsible for Mg^{2+}-dependent $3' \rightarrow 5'$ processive phosphorolytic degradation of RNA and template-independent polymerization of rNDPs into RNA (31–36). It is likely that PNPase plays a dual role in response to genotoxic agents, participating both in RNA turn-over (31–36) and in facilitating DNA DSB repair (27). It emerges that PNPase is a versatile enzyme that can be directed toward either RNA or DNA metabolism by metal ions. Its reversible activity not only is determined by substrate (Pi and r/dNDP's) concentration, but also is modulated by nucleotide triphosphates cofactors and can associate with different proteins to build up machines dedicated to cellular functions apparently as diverse as RNA turnover and DNA repair and recombination (9,27).

Genetic data suggest that PNPase$_{Bsu}$ is required for repair of H_2O_2-induced DSB repair via RecN-dependent HR or Ku-dependent NHEJ, whereas it is dispensable for MMC-induced DSB repair (27). H_2O_2-induced DSB can chemically alter DNA ends, whereas MMC-induced crosslinks and subsequently the generated DNA DSBs have clean ends. It is likely that PNPase plays an active role when the ends are chemically modified although the resection reaction may proceed more slowly. A similar role has been attributed to Mre11 [reviewed by (5)]. Our cytological results suggest that PNPase$_{Bsu}$ is not involved in RecN foci formation. RecN forms a discrete focus per nucleoid in *pnpA*$^+$ cells and few foci and patchy structures in *pnpA*$^-$ cells (Figure 1). A similar effect was observed in the absence of long-range resection in the *addA* and Δ*recJ* background (24), suggesting that PNPase$_{Bsu}$, which co-purifies with RecN (27), contributes to RecN-mediated RCs before and/or concomitantly with long-range end-processing by the AddAB or the RecJ-RecQ/RecS enzymes. This is consistent with the observation that Δ*pnpA* is epistatic to the Δ*recN* or Δ*ku* mutations, which by themselves are non-epistatic, whereas Δ*pnpA* is non-epistatic to *addA* or Δ*recJ* (27).

Our biochemical results demonstrate that RecN stimulates Mn^{2+}-dependent PNPase$_{Bsu}$ polymerization on 3′-OH ends. It is likely that RecN, by binding to 3′-OH ends in an ATP-dependent manner and tethering and

bridging them (26), facilitates PNPase-mediated template-independent polymerization (Figure 5A and Supplementary Figure S7A) at the local high concentration of DNA ends (rosette-like structures). RecA, even in the dADP bound form, promotes disassembly of the RecN-induced rosette-like structures and stimulates Mn^{2+}-dependent $3' \rightarrow 5'$ degradation of ssDNA by $PNPase_{Bsu}$ (Figure 6A and Supplementary Figure S7B). Many bacteria accumulate Mn^{2+}, and high intracellular levels of Mn^{2+} directly or indirectly allow fast repair of damaged DNA after DSBs (61,62).

A molecular model for PNPase role in DSB repair

What could be the mechanistic role of PNPase? The responses of eukaryotic and bacterial cells to DNA DSBs show some similarities and clear differences. The eukaryotic MRN(X) complex and bacterial RecN are among the first responders to DNA DSBs (10,22,63); both Rad50, as part of the MRN(X) complex, and RecN bind to the DNA ends in an ATP-dependent manner and tether and bridge them (25,26). $PNPase_{Bsu}$, which might work at early stages of DNA DSB repair process, may be implicated in the repair of two-ended DSBs that are created by H_2O_2, which leaves non-ligatable termini. This is consistent with the observation that a *pnpA* mutation is epistatic to *recN* and *ku* mutations, which by themselves are non-epistatic (27). Biochemical analyses suggested that in the presence of Mn^{2+} and dNDPs, PNPase elongates short 3′-protruding, blunt or, with lower efficiency, 3′-recessive ends. In the dATP bound form, RecN enhances $PNPase_{Bsu}$ polymerization even on SsbA-coated ssDNA. It is likely that the RecN interaction with the PNPase-extended 3′-OH ends and SsbA bound to the recombinogenic 3′-ssDNA regions limit the access of the Ku protein to the DNA ends, thus directing the reaction towards error-free DSB repair via HR. This is consistent with the observation that: (i) RecN bound to the 3′-OH ends protects them from ExoIII degradation (50), but facilitates PNPase-mediated extension of the 3′-OHs, and (ii) $PNPase_{Bsu}$, by adding template independent tails to a DSB end might block NHEJ and indirectly constitutes a control point in DNA repair via HR. In contrast, in the absence of RecN and long-range end processing, $PNPase_{Bsu}$, or any other ssDNA exonuclease, might degrade the 3′-OHs and indirectly facilitate Ku-mediated NHEJ, suggesting that PNPase might contribute in repair pathway choice. This is consistent with the observation that Δ*pnpA* and Δ*ku* are epistatic (27).

Is end processing conserved among bacteria? *B. subtilis* RecN is essential for the repair of DNA breaks (64). Like $PNPase_{Bsu}$ (see above), *E. coli* RecN is dispensable for the repair of 'clean' breaks created by *EcoR*I endonuclease (65), but essential for the repair of breaks created by ionizing radiation or bleomycin (66,67), which can chemically alter DNA ends (68). It is likely that bacterial RecN in concert with PNPase plays an active role when the ends are chemically modified. Similarly to the MRX(N)-Sae2(CtIP) complex (15,17,69), $PNPase_{Bsu}$ might contribute to the formation of an early intermediate for long-range end resection. Both Mre11 (11–14) and $PNPase_{Bsu}$ (27, this work) show an Mn^{2+}-dependent $3' \rightarrow 5'$ exonuclease activity. PNPase degradation was observed with 3′-tailed duplex DNA (Figure 2), whereas degradation was inefficient or it did not occur on a 3′-recessed end (Figure 4A). In *E. coli*, PNPase co-purifies with RecA (58). RecA stimulates PNPase 3′-end degradation by a mechanism that neither requires ATP hydrolysis nor formation of an active filament. This stimulatory effect on PNPase-mediated degradation ssDNA takes place even in the absence of a 3′-OH end. This basal end processing might facilitate the removal of 'non-ligatable' 3′-ends prior to long-range resection of the 5′ strand of DNA by RecJ-RecQ/RecS or the AddAB complex. $PNPase_{Bsu}$ degradation of 3′-ends might contribute to process the 3′-tailed ends derived from collapsed replication forks with nicks on the lagging strand, because end-processing by the AddAB(RecBCD) complex requires blunt or nearly blunt ends (23). This is consistent with the observation that *B. subtilis* lacks many $3' \rightarrow 5'$ ssDNA exonucleases (such as ExoI, ExoIX or ExoX) that are present in *E. coli* (27).

Based on our results we propose that in *B. subtilis* RecA plays an early role in DSB repair by dislodging RecN from the overhangs of duplex DNA molecules (26,50) and promoting PNPase degradation prior to long-range resection. However, the potential implication of PNPase alone or in concert with RecA in the generation of the proper substrate for AddAB or RecJ-RecQ/RecS activity remains to be addressed (26,27,50).

PNPase activity is modulated by (d/rATP)

A nucleotide triphosphate allosterically inhibits all PNPase activities on RNA and ssDNA (46, this work), but its hydrolysis products are substrates for phosphorolytic degradation (Pi) and polymerization (r/dADP) on both RNA and ssDNA substrates (27,31,33, this work). The RecN and RecA modulators of $PNPase_{Bsu}$ activities on ssDNA are genuine ssDNA-dependent ATPases (21,50) that lower the local concentration of the nucleotide triphosphate and therefore release the allosteric inhibition. This fits with the previously proposed idea that RNA helicases (which share a RecA-like motif) associated with PNPase at the degradosome may modulate PNPase activities by decreasing the local concentration of ATP (46).

SUPPLEMENTARY DATA

Supplementary Data are available at NAR Online

ACKNOWLEDGEMENTS

The authors thank P.L. Graumann for introducing us in the field of fluorescence microscopy, D. Bechhofer for plasmid-borne *pnpA* gene, and L. Blanco for critical reading of the manuscript.

FUNDING

Funding for open access charge: Ministero dell'Università e della Ricerca and Università degli Studi di Milano (PRIN 2007 - 20074CNBJ2); and Universitàdegli Studi di Milano (FIRST 2007 and PUR 2008) (to G.D.).

Conflict of interest statement. None declared.

REFERENCES

1. Pâques,F. and Haber,J.E. (1999) Multiple pathways of recombination induced by double-strand breaks in *Saccharomyces cerevisiae*. *Microbiol. Mol. Biol. Rev.*, **63**, 349–404.
2. Shuman,S. and Glickman,M.S. (2007) Bacterial DNA repair by non-homologous end joining. *Nat. Rev. Microbiol.*, **5**, 852–861.
3. Aguilera,A. and Gomez-Gonzalez,B. (2008) Genome instability: a mechanistic view of its causes and consequences. *Nat. Rev. Genet.*, **9**, 204–217.
4. Lisby,M. and Rothstein,R. (2009) Choreography of recombination proteins during the DNA damage response. *DNA Repair*, **8**, 1068–1076.
5. Mimitou,E.P. and Symington,L.S. (2009) Nucleases and helicases take center stage in homologous recombination. *Trends Biochem. Sci.*, **34**, 264–272.
6. Niu,H., Raynard,S. and Sung,P. (2009) Multiplicity of DNA end resection machineries in chromosome break repair. *Genes Dev.*, **23**, 1481–1486.
7. San Filippo,J., Sung,P. and Klein,H. (2008) Mechanism of eukaryotic homologous recombination. *Annu. Rev. Biochem.*, **77**, 229–257.
8. Huertas,P. (2010) DNA resection in eukaryotes: deciding how to fix the break. *Nat. Struct. Mol. Biol.*, **17**, 11–16.
9. Ayora,S., Carrasco,B., Cardenas,P.P., Cesar,C.E., Cañas,C., Yadav,T., Marchisone,C. and Alonso,J.C. (2011) Double-strand break repair in bacteria: a view from *Bacillus subtilis*. *FEMS Microbiol. Rev*, 2011 Apr 25. doi: 10.1111/j.1574-6976.2011.00272.x. [Epub ahead of print] PMID: 21517913.
10. Stracker,T.H., Theunissen,J.W., Morales,M. and Petrini,J.H. (2004) The Mre11 complex and the metabolism of chromosome breaks: the importance of communicating and holding things together. *DNA Repair*, **3**, 845–854.
11. Paull,T.T. and Gellert,M. (1998) The 3′ to 5′ exonuclease activity of Mre 11 facilitates repair of DNA double-strand breaks. *Mol. Cell.*, **1**, 969–979.
12. Trujillo,K.M., Yuan,S.S., Lee,E.Y. and Sung,P. (1998) Nuclease activities in a complex of human recombination and DNA repair factors Rad50, Mre11, and p95. *J. Biol. Chem.*, **273**, 21447–21450.
13. Lengsfeld,B.M., Rattray,A.J., Bhaskara,V., Ghirlando,R. and Paull,T.T. (2007) Sae2 is an endonuclease that processes hairpin DNA cooperatively with the Mre11/Rad50/Xrs2 complex. *Mol. Cell.*, **28**, 638–651.
14. Sartori,A.A., Lukas,C., Coates,J., Mistrik,M., Fu,S., Bartek,J., Baer,R., Lukas,J. and Jackson,S.P. (2007) Human CtIP promotes DNA end resection. *Nature*, **450**, 509–514.
15. Mimitou,E.P. and Symington,L.S. (2008) Sae2, Exo1 and Sgs1 collaborate in DNA double-strand break processing. *Nature*, **455**, 770–774.
16. Gravel,S., Chapman,J.R., Magill,C. and Jackson,S.P. (2008) DNA helicases Sgs1 and BLM promote DNA double-strand break resection. *Genes Dev.*, **22**, 2767–2772.
17. Zhu,Z., Chung,W.H., Shim,E.Y., Lee,S.E. and Ira,G. (2008) Sgs1 helicase and two nucleases Dna2 and Exo1 resect DNA double-strand break ends. *Cell*, **134**, 981–994.
18. Cejka,P., Cannavo,E., Polaczek,P., Masuda-Sasa,T., Pokharel,S., Campbell,J.L. and Kowalczykowski,S.C. (2010) DNA end resection by Dna2-Sgs1-RPA and its stimulation by Top3-Rmi1 and Mre11-Rad50-Xrs2. *Nature*, **467**, 112–116.
19. Niu,H., Chung,W.H., Zhu,Z., Kwon,Y., Zhao,W., Chi,P., Prakash,R., Seong,C., Liu,D., Lu,L. *et al.* (2010) Mechanism of the ATP-dependent DNA end-resection machinery from *Saccharomyces cerevisiae*. *Nature*, **467**, 108–111.
20. Nimonkar,A.V., Genschel,J., Kinoshita,E., Polaczek,P., Campbell,J.L., Wyman,C., Modrich,P. and Kowalczykowski,S.C. (2011) BLM-DNA2-RPA-MRN and EXO1-BLM-RPA-MRN constitute two DNA end resection machineries for human DNA break repair. *Genes Dev.*, **25**, 350–362.
21. Cox,M.M. (2007) Motoring along with the bacterial RecA protein. *Nat. Rev. Mol. Cell. Biol.*, **8**, 127–138.
22. Kidane,D., Sanchez,H., Alonso,J.C. and Graumann,P.L. (2004) Visualization of DNA double-strand break repair in live bacteria reveals dynamic recruitment of *Bacillus subtilis* RecF, RecO and RecN proteins to distinct sites on the nucleoids. *Mol. Microbiol.*, **52**, 1627–1639.
23. Yeeles,J.T. and Dillingham,M.S. (2010) The processing of double-stranded DNA breaks for recombinational repair by helicase-nuclease complexes. *DNA Repair*, **9**, 276–285.
24. Sanchez,H., Kidane,D., Cozar,M.C., Graumann,P.L. and Alonso,J.C. (2006) Recruitment of *Bacillus subtilis* RecN to DNA double-strand breaks in the absence of DNA end processing. *J. Bacteriol.*, **188**, 353–360.
25. Moreno-Herrero,F., de Jager,M., Dekker,N.H., Kanaar,R., Wyman,C. and Dekker,C. (2005) Mesoscale conformational changes in the DNA-repair complex Rad50/Mre11/Nbs1 upon binding DNA. *Nature*, **437**, 440–443.
26. Sanchez,H., Cardenas,P.P., Yoshimura,S.H., Takeyasu,K. and Alonso,J.C. (2008) Dynamic structures of *Bacillus subtilis* RecN-DNA complexes. *Nucleic Acids Res.*, **36**, 110–120.
27. Cardenas,P.P., Carrasco,B., Sanchez,H., Deikus,G., Bechhofer,D.H. and Alonso,J.C. (2009) *Bacillus subtilis* polynucleotide phosphorylase 3'-to-5' DNase activity is involved in DNA repair. *Nucleic Acids Res.*, **37**, 4157–4169.
28. Sinha,K.M., Unciuleac,M.C., Glickman,M.S. and Shuman,S. (2009) AdnAB: a new DSB-resecting motor-nuclease from mycobacteria. *Genes Dev.*, **23**, 1423–1437.
29. Tomita,K., Matsuura,A., Caspari,T., Carr,A.M., Akamatsu,Y., Iwasaki,H., Mizuno,K., Ohta,K., Uritani,M., Ushimaru,T. *et al.* (2003) Competition between the Rad50 complex and the Ku heterodimer reveals a role for Exo1 in processing double-strand breaks but not telomeres. *Mol. Cell. Biol.*, **23**, 5186–5197.
30. Wasko,B.M., Holland,C.L., Resnick,M.A. and Lewis,L.K. (2009) Inhibition of DNA double-strand break repair by the Ku heterodimer in *mrx* mutants of *Saccharomyces cerevisiae*. *DNA Repair*, **8**, 162–169.
31. Condon,C. (2003) RNA processing and degradation in *Bacillus subtilis*. *Microbiol. Mol. Biol. Rev.*, **67**, 157–174.
32. Grunberg-Manago,M. (1999) Messenger RNA stability and its role in control of gene expression in bacteria and phages. *Annu. Rev. Genet.*, **33**, 193–227.
33. Ochoa,S. (1957) Enzymic synthesis of polynucleotides. III. Phosphorolysis of natural and synthetic ribopolynucleotides. *Arch. Biochem. Biophys.*, **69**, 119–129.
34. Mohanty,B.K. and Kushner,S.R. (2000) Polynucleotide phosphorylase functions both as a $3' \rightarrow 5'$ exonuclease and a poly(A) polymerase in *Escherichia coli*. *Proc. Natl Acad. Sci. USA*, **97**, 11966–11971.
35. Campos-Guillen,J., Bralley,P., Jones,G.H., Bechhofer,D.H. and Olmedo-Alvarez,G. (2005) Addition of poly(A) and heteropolymeric 3' ends in *Bacillus subtilis* wild-type and polynucleotide phosphorylase-deficient strains. *J. Bacteriol.*, **187**, 4698–4706.
36. Sarkar,D. and Fisher,P.B. (2006) Polynucleotide phosphorylase: an evolutionary conserved gene with an expanding repertoire of functions. *Pharmacol Ther*, **112**, 243–263.
37. Deutscher,M.P. and Reuven,N.B. (1991) Enzymatic basis for hydrolytic versus phosphorolytic mRNA degradation in *Escherichia coli* and *Bacillus subtilis*. *Proc. Natl Acad. Sci. USA*, **88**, 3277–3280.
38. Kushner,S.R. (1996) mRNA decay. In Neidhardt,F.C. (ed.), *Escherichia coli and Salmonella cellular and molecular Biology*. ASM Press, Washington DC, pp. 849–860.
39. Chou,J.Y. and Singer,M.F. (1971) Deoxyadenosine diphosphate as a substrate and inhibitor of polynucleotide phosphorylase of *Micrococcus luteus*. II. Inhibition of the initiation of adenosine

diphosphate polymerization by deoxyadenosine diphosphate. *J. Biol. Chem.*, **246**, 7497–7504.
40. Gillam,S. and Smith,M. (1974) Enzymatic synthesis of deoxyribo-oligonucleotides of defined sequence. Properties of the enzyme. *Nucleic Acids Res.*, **1**, 1631–1647.
41. Beljanski,M. (1996) *de novo* synthesis of DNA-like molecules by polynucleotide phosphorylase *in vitro*. *J. Mol. Evol.*, **42**, 493–499.
42. Wu,J., Jiang,Z., Liu,M., Gong,X., Wu,S., Burns,C.M. and Li,Z. (2009) Polynucleotide phosphorylase protects *Escherichia coli* against oxidative stress. *Biochemistry*, **48**, 2012–2020.
43. Regonesi,M.E., Briani,F., Ghetta,A., Zangrossi,S., Ghisotti,D., Tortora,P. and Dehò,G. (2004) A mutation in polynucleotide phosphorylase from *Escherichia coli* impairing RNA binding and degradosome stability. *Nucleic Acids Res.*, **32**, 1006–1017.
44. Sperandeo,P., Pozzi,C., Dehò,G. and Polissi,A. (2006) Non-essential KDO biosynthesis and new essential cell envelope biogenesis genes in the *Escherichia coli yrbG-yhbG* locus. *Res. Microbiol.*, **157**, 547–558.
45. Jarrige,A., Brechemier-Baey,D., Mathy,N., Duche,O. and Portier,C. (2002) Mutational analysis of polynucleotide phosphorylase from *Escherichia coli*. *J. Mol. Biol.*, **321**, 397–409.
46. Del Favero,M., Mazzantini,E., Briani,F., Zangrossi,S., Tortora,P. and Dehò,G. (2008) Regulation of *Escherichia coli* polynucleotide phosphorylase by ATP. *J. Biol. Chem.*, **283**, 27355–27359.
47. Deikus,G. and Bechhofer,D.H. (2007) Initiation of decay of *Bacillus subtilis trp* leader RNA. *J. Biol. Chem.*, **282**, 20238–20244.
48. Carrasco,B., Manfredi,C., Ayora,S. and Alonso,J.C. (2008) *Bacillus subtilis* SsbA and dATP regulate RecA nucleation onto single-stranded DNA. *DNA Repair*, **7**, 990–996.
49. Carrasco,B., Ayora,S., Lurz,R. and Alonso,J.C. (2005) *Bacillus subtilis* RecU Holliday-junction resolvase modulates RecA activities. *Nucleic Acids Res.*, **33**, 3942–3952.
50. Sanchez,H. and Alonso,J.C. (2005) *Bacillus subtilis* RecN binds and protects 3′-single-stranded DNA extensions in the presence of ATP. *Nucleic Acids Res.*, **33**, 2343–2350.
51. Arenghi,F.L., Barbieri,P., Bertoni,G. and de Lorenzo,V. (2001) New insights into the activation of o-xylene biodegradation in *Pseudomonas stutzeri* OX1 by pathway substrates. *EMBO Rep.*, **2**, 409–414.
52. Taghbalout,A. and Rothfield,L. (2008) RNaseE and RNA helicase B play central roles in the cytoskeletal organization of the RNA degradosome. *J. Biol. Chem.*, **283**, 13850–13855.
53. Littauer,U.Z. and Grunberg-Manago,M. (1999) *Polynucleotide Phosphorylase*. John Wiley and Sons, New York.
54. Bermudez-Cruz,R.M., Garcia-Mena,J. and Montañez,C. (2002) Polynucleotide phosphorylase binds to ssRNA with same affinity as to ssDNA. *Biochimie*, **84**, 321–328.
55. Egelman,E.H. and Stasiak,A. (1986) Structure of helical RecA-DNA complexes. Complexes formed in the presence of ATPγS or ATP. *J. Mol. Biol.*, **191**, 677–697.
56. Heuser,J. and Griffith,J. (1989) Visualization of RecA protein and its complexes with DNA by quick-freeze/deep-etch electron microscopy. *J. Mol. Biol.*, **210**, 473–484.
57. Lovett,C.M. Jr. and Roberts,J.W. (1985) Purification of a RecA protein analogue from *Bacillus subtilis*. *J. Biol. Chem.*, **260**, 3305–3313.
58. Register,J.C. 3rd and Griffith,J. (1985) 10 nm RecA protein filaments formed in the presence of Mg^{2+} and ATPγS may contain RNA. *Mol. Gen. Genet.*, **199**, 415–420.
59. Lehnik-Habrink,M., Pfortner,H., Rempeters,L., Pietack,N., Herzberg,C. and Stulke,J. (2011) The RNA degradosome in Bacillus subtilis: identification of CshA as the major RNA helicase in the multiprotein complex. *Mol. Microbiol.*, **77**, 958–971.
60. Galletto,R. and Kowalczykowski,S.C. (2007) RecA. *Curr. Biol.*, **17**, R395–R397.
61. Daly,M.J., Gaidamakova,E.K., Matrosova,V.Y., Vasilenko,A., Zhai,M., Leapman,R.D., Lai,B., Ravel,B., Li,S.M., Kemner,K.M. *et al.* (2007) Protein oxidation implicated as the primary determinant of bacterial radioresistance. *PLoS Biol.*, **5**, e92.
62. Daly,M.J., Gaidamakova,E.K., Matrosova,V.Y., Vasilenko,A., Zhai,M., Venkateswaran,A., Hess,M., Omelchenko,M.V., Kostandarithes,H.M., Makarova,K.S. *et al.* (2004) Accumulation of Mn(II) in *Deinococcus radiodurans* facilitates γ-radiation resistance. *Science*, **306**, 1025–1028.
63. Lisby,M., Barlow,J.H., Burgess,R.C. and Rothstein,R. (2004) Choreography of the DNA damage response: spatiotemporal relationships among checkpoint and repair proteins. *Cell*, **118**, 699–713.
64. Alonso,J.C., Stiege,A.C. and Luder,G. (1993) Genetic recombination in *Bacillus subtilis* 168: effect of *recN*, *recF*, *recH* and *addAB* mutations on DNA repair and recombination. *Mol. Gen. Genet.*, **239**, 129–136.
65. Heitman,J., Zinder,N.D. and Model,P. (1989) Repair of the *Escherichia coli* chromosome after *in vivo* scission by the *Eco*RI endonuclease. *Proc. Natl Acad. Sci. USA*, **86**, 2281–2285.
66. Kosa,J.L., Zdraveski,Z.Z., Currier,S., Marinus,M.G. and Essigmann,J.M. (2004) RecN and RecG are required for *Escherichia coli* survival of Bleomycin-induced damage. *Mutat. Res.*, **554**, 149–157.
67. Picksley,S.M., Attfield,P.V. and Lloyd,R.G. (1984) Repair of DNA double-strand breaks in *Escherichia coli* K12 requires a functional *recN* product. *Mol. Gen. Genet.*, **195**, 267–274.
68. Henner,W.D., Rodriguez,L.O., Hecht,S.M. and Haseltine,W.A. (1983) γ-Ray induced deoxyribonucleic acid strand breaks. 3′ Glycolate termini. *J. Biol. Chem.*, **258**, 711–713.
69. Hopkins,B.B. and Paull,T.T. (2008) The *P. furiosus* Mre11/Rad50 complex promotes 5' strand resection at a DNA double-strand break. *Cell*, **135**, 250–260.